Chemical Physics Letters 784 (2021) 139099

Contents lists available at ScienceDirect

Chemical Physics Letters

journal homepage: www.elsevier.com/locate/cplett

Research paper

Accurate calculations for the Dirac electron in the field of two-center Coulomb field: Application to heavy ions

O. Chuluunbaatar [a,b], B.B. Joulakian [c,*], G. Chuluunbaatar [a,d], J. Buša Jr [a,e], G.O. Koshcheev [a,f]

[a] Joint Institute for Nuclear Research, Dubna, Moscow Region 141980, Russia
[b] Institute of Mathematics and Digital Technology, Mongolian Academy of Sciences, Ulaanbaatar 13330, Mongolia
[c] Université de Lorraine, LPCT (UMR CNRS 7019), 1 bld Arago, bat. ICPM 57078 Metz Cedex 3, France
[d] Peoples' Friendship University of Russia (RUDN University), 117198 Moscow, Russia
[e] Institute of Experimental Physics, Slovak Academy of Sciences, Watsonova 47, 040 01 Košice, Slovakia
[f] Institute of System Analysis and Management, Dubna State University, Dubna, Moscow Region 141980, Russia

ARTICLE INFO

Keywords:
Dirac two center problem
Spurious solutions
Negative energy levels fo heavy ions
Relativistic Slater spinors
Minimax procedure

ABSTRACT

The relativistic Dirac equation for a bound electron in the field of two fixed positive charges is revisited. In contrast to the one center case this three dimensional equation is separable only partially around the azimuthal angle φ, because of the commutation of the Dirac Hamiltonian only with the z component of the total angular momentum J_z. In this work we determine the variational exact solution of this two center problem using a basis constructed by linear combinations of relativistic Slater type spinor wave functions with non integer powers of the radii r_1 and r_2 on the two centers. We present in some detail the determination of the two center integrations involved. The solutions are obtained by a minimax procedure, that we have developed with a new iterative scheme. We use independent large and small components of the Dirac spinor. This permits us to take control of the spurious solutions, and gives us the possibility to avoid them by the appropriate choice of the wave function parameters. We investigate the behavior of the electron in its $1s\sigma_g$ level of the diatomic homo-nuclear systems $A_2^{(2Z-1)+}$, where A represents the heavy element and Z its atomic number. In the case of heavy ions we study the dependance of the electron energy on the internuclear distance, this gives us an indication for the conditions of atomic collapse, which can induce electron-positron pair production. Our approach has the advantage of needing small basis sets for a relative error of the of $10^{-7}-10^{-8}$. It can also be extended easily to the excited level such as the $1s\sigma_u$ level.

1. Introduction

The relativistic Dirac equation for an electron in the field of two fixed positive charges is one of the basic problems of quantum mechanics. In contrast to the non relativistic case, which is separable in prolate spheroidal coordinates [1,2], owing to the existence of the Coulson constant of separation, which was obtained by Coulson [3] from the Runge-Lenz vector, the relativistic case is not separable. An equivalent relativistic constant of separation could not be obtained from the Lipmann operator [4], which is the relativistic analogue of the Runge-Lenz vector. The only possible separation is that of the azimuthal angle φ which results from the commutation of the two-center Dirac Hamiltonian with the z component of the total angular momentum $J_z = L_z + \sigma_z/2$.

Finding a reliable solution of the two-center Dirac equation is essential in many domains of relativistic studies of diatomic systems. The solutions of the Dirac equation characterize, in contrast to the relativistic Schrödinger or the Pauli equations, positive and negative energy states, which can be observed in collisions of heavy nuclei [5]. The spin and other relativistic aspects are also characterized by the solutions of the Dirac equation. The energy value $E_R = E_e + m_e c^2$ of an electron described by a Dirac hamiltonian, where E_e represent the binding or the kinetic energy of the electron, can be found in one of the following domains. It can be in the negative energy continuum $E_R < -m_e c^2$, in the the bound energy domain $-m_e c^2 < E_R < m_e c^2$ and in the free electron energy region $E_R > m_e c^2$. As E_e of the diatomic system depends on the nuclear charges and the internuclear distance between the two nuclei, it will decrease, when the two nuclei are brought near to

* Corresponding author.
E-mail address: Boghos.Joulakian@univ-lorraine.fr (B.B. Joulakian).

https://doi.org/10.1016/j.cplett.2021.139099
Received 11 June 2021; Received in revised form 15 September 2021; Accepted 29 September 2021
Available online 5 October 2021

each other in ion-ion collisions. In some extreme cases, when the charges of the nuclei are high enough, the energy can arrive to the negative continuum region. In this situation the system goes into a resonant state, where an electron-positron pair is produced, by the passage of the electron to the positive energy continuum [6,7].

This unusual atomic collapse situation can also be obtained, when highly charged impurities are introduced in graphene. Although our main aim in this work is to create a numerical tool to calculate reliable solutions for the Dirac equation of an individual electron in the field of two fixed positive charges, it would be useful to mention other relativistic studies concerned with atomic collapse. These studies employ two dimensional Dirac equation. In [8] the supercritical instability in graphene is studied when two charged impurities are introduced in it. In [9] the electric dipole effects for massive Dirac fermions in graphene and related materials is analyzed. In [10] a variational method is applied for the determination of the critical distance between two Coulomb centers in Graphene. In [11,12] the Dirac equation for quasiparticles in gapped graphene with two oppositely charged impurities is studied by using the technique of linear combination of atomic orbitals. In [13] the study goes on the scattering theory and ground-state energy determination of Dirac fermions in graphene with two Coulomb impurities. More details on the electronic states created by two impurities in Graphene and the application of the Dirac equation can be found in [14].

Concerning the two center one electron original Dirac equation, many attempts have been made to find appropriate solutions of this problem. From the long list of publications on this subject, we can chose some typical ones. We begin by the application of the simple LCAO trial spinor wave function [15]. In this approximation the first component of the Dirac spinor was replaced by the nonrelativistic $1s$ function. In another attempt, a spinor was constructed in which the four components were represented each by a series of spheroidal functions borrowed from the non relativistic case [16]. The Gaussian lobe functions were employed in [17] to calculate the relativistic correction for the energy of H_2^+. The convergence of the solution in Gaussian linear expansion spinors was investigated numerically in [18]. For large internuclear distances the resonance between $1s\sigma_g$ and $1s\sigma_u$ levels was studied in [19]. The minimax variational principle was applied to solve the variational problem in [20,21]. In [22] an analytic expansion applying an iterative variational method was applied. In [23], highly accurate finite element calculations were performed for the ground state of Th_2^{179+}. B-spline basis sets, constructed in Cassini coordinates were applied in [24]. In [25] Tupitsyn et al. developed a method for solving the stationary two-center Dirac equation using wave functions represented as series of atomic like Dirac-Sturm orbitals, localized on the ions. Here, the atomic orbitals are generated by solving numerically the one-center Dirac and Dirac-Sturm equations by means of a finite-difference approach. The problem is solved for many nuclear charges and compared to existing results H_2^+, Th_2^{179+} and U_2^{193+} at the "chemical" internuclear distance $\rho = 2/Z$.

In all the above cited variational methods the main encountered difficulty is the appearance of spurious solutions. These correspond to solutions of the Dirac equation for which the energy value of the fundamental level is lower than the exact value. This violates the variation principle, as the variational result should always be an upper limit of the exact value of the energy [26]. The origin of this difficulty is the existence of the negative energy continuum $E_R < -m_e c^2$ in the spectrum of the Dirac electron. In [27,28] the mechanism of the appearance of these solutions is analyzed and some judicious artificial numerical methods are proposed to avoid them. In our present approach, we have taken profit of the above cited experiences in the computational domain. We have identified the particular situations and the parameters of the trial wave function for which the undesired spurious solutions appear and have succeeded in avoiding them.

In our present approach, we have applied Slater-type spinor orbitals with non-integer principal quantum numbers (NISTOs) [29,20,21] centered on the nuclei. This has necessitated the creation of an efficient algorithm for the determination of two-center integrals with high accuracy. We have imposed correct Coulomb asymptotic behavior for the cases of near and far nuclei. We have realized, with relatively smaller basis sets, the same precision as that obtained by past calculations using hundreds of Gaussian basis functions for heavy ions. We have also used trial spinors with independent large and small components. This imposes the use of the minimax procedure instead of the habitual minimization methods. Many algorithms and methods are available to realize the calculation for the convex-concave minimax problem (or for Nash equilibrium). There are also several package programs for the discrete minimax problem, for example FSQP code [30], but there are no package programs for the continuous minimax problem. We have therefore developed a new iterative scheme based on Newton-type minimization method [31] and continuous minimax [32] problems in combination with negative curvature direction methods for non-convex-non-concave, convex-non-concave and non-convex-concave cases [31,33]. We have also used the optimal steps of the Newton-type method like in [34]. We intend to give these details in a separate paper. As it will be shown below, the comparison of the parameters used for the large and small components permitted us to identify the spurious solutions and make the right choice of the parameters to avoid these undesirable solutions.

2. Theory

The one-electron wave function $\Psi(\vec{r})$ is a solution of the stationary Dirac equation

$$H_D\Psi(\vec{r}) = E\Psi(\vec{r}), \tag{1}$$

where $E = E_R$ is the relativistic energy, and H_D is the two-center Dirac hamiltonian in atomic units ($e = m_e = \hbar = 1$):

$$H_D = c\,\vec{\alpha}\,\vec{p} + c^2\beta + U(\vec{r})\mathbf{I}. \tag{2}$$

Here c is the speed of light, $\vec{\alpha}$ and β are Dirac matrices:

$$\begin{gathered}\vec{\alpha} = \begin{pmatrix} 0 & \vec{\sigma} \\ \vec{\sigma} & 0 \end{pmatrix}, \quad \vec{\sigma} = \left(\sigma_x, \sigma_y, \sigma_z\right), \quad \beta = \begin{pmatrix} I & 0 \\ 0 & -I \end{pmatrix}, \\ \sigma_x = \begin{pmatrix} 0 & 1 \\ 1 & 0 \end{pmatrix}, \quad \sigma_y = \begin{pmatrix} 0 & -\imath \\ \imath & 0 \end{pmatrix}, \quad \sigma_z = \begin{pmatrix} 1 & 0 \\ 0 & -1 \end{pmatrix},\end{gathered} \tag{3}$$

$$\mathbf{I} = \begin{pmatrix} I & 0 \\ 0 & I \end{pmatrix}, \quad I = \begin{pmatrix} 1 & 0 \\ 0 & 1 \end{pmatrix}.$$

The two-center attractive Coulomb potential $U(\vec{r})$ is defined by

$$U\left(\vec{r}\right) = V\left(r_1\right) + V\left(r_2\right), \quad V\left(r\right) = -\frac{Z}{r},$$

where Z is the point charge of the centers 1 and 2, $\vec{r}_1 = \vec{r} + \vec{\rho}/2, \vec{r}_2 = \vec{r} - \vec{\rho}/2, \vec{\rho} = (0,0,\rho)$, and ρ is the internuclear distance.

The Slater-type spinor orbitals centered on the nuclei are given as in [29] by

$$\psi_{njlm}\left(\vec{r}\right) \equiv \psi_{n\kappa m}\left(\vec{r}\right) = \begin{cases} \imath P_{n\kappa}(r)\Omega_{+\kappa m}(\theta,\varphi) \\ Q_{n\kappa}(r)\Omega_{-\kappa m}(\theta,\varphi). \end{cases} \tag{4}$$

Here the spinor spherical harmonics

$$\Omega_{jlm}\begin{pmatrix}\theta,\varphi\end{pmatrix} \equiv \Omega_{\kappa m}\begin{pmatrix}\theta,\varphi\end{pmatrix} = \begin{cases} \begin{cases} +\sqrt{\dfrac{l+m+1/2}{2l+1}}\,Y_{lm-1/2}\left(\theta,\varphi\right), \\ +\sqrt{\dfrac{l-m+1/2}{2l+1}}\,Y_{lm+1/2}\left(\theta,\varphi\right), \end{cases} & \kappa<0, \quad l=-\kappa-1, \\ \begin{cases} -\sqrt{\dfrac{l-m+1/2}{2l+1}}\,Y_{lm-1/2}\left(\theta,\varphi\right), \\ +\sqrt{\dfrac{l+m+1/2}{2l+1}}\,Y_{lm+1/2}\left(\theta,\varphi\right), \end{cases} & \kappa>0, \quad l=\kappa, \end{cases} \qquad j=|\kappa|-1\Big/2, \tag{5}$$

are eigenfunctions of the operator $\overrightarrow{\sigma}\overrightarrow{L}$:

$$\left(-\overrightarrow{\sigma}\overrightarrow{L}-I\right)\Omega_{\kappa m}\left(\theta,\varphi\right)=\kappa\Omega_{\kappa m}\left(\theta,\varphi\right), \tag{6}$$

where $\overrightarrow{L}$ is the orbital angular momentum, and $Y_{lm}(\theta,\varphi)$ is the spherical harmonic, according to the Condon and Shortley phase convention [35]. The spinor spherical harmonics satisfy the following equations:

$$\overrightarrow{\sigma}\widehat{r}\,\Omega_{+m}(\theta,\varphi)=-\Omega_{-\kappa m}(\theta,\varphi), \quad \widehat{r}=\overrightarrow{r}/r, \tag{7}$$

$$\overrightarrow{\sigma}\overrightarrow{p}\,\Omega_{+\kappa m}\left(\theta,\varphi\right)=\imath\left(\frac{\partial}{\partial r}+\frac{1+\kappa}{r}\right)\Omega_{-\kappa m}\left(\theta,\varphi\right). \tag{8}$$

When the potential $U(\overrightarrow{r})\equiv V(r)$ is spherically symmetrical, the large $P_{n\kappa}(r)$ and small $Q_{n\kappa}(r)$ radial components satisfy the following coupled equations

$$\begin{aligned} &+c\left[\frac{\partial}{\partial r}+\frac{1-\kappa}{r}\right]Q_{n\kappa}\left(r\right)+\left(V\left(r\right)+c^2-E_{n\kappa}\right)P_{n\kappa}\left(r\right)=0, \\ &-c\left[\frac{\partial}{\partial r}+\frac{1+\kappa}{r}\right]P_{n\kappa}\left(r\right)+\left(V\left(r\right)-c^2-E_{n\kappa}\right)Q_{n\kappa}\left(r\right)=0. \end{aligned} \tag{9}$$

The particularity of our approach is that, for the two-center problem considered, the one center basis large $P_{n\kappa}(r)$ and small $Q_{n\kappa}(r)$ radial components located on each center are chosen in the form

$$\begin{aligned} P_{n\kappa}\left(r\right)&=(-1)^l\sum_{n_p=1}^{n_{p\max}}c_{n_p\kappa}p_{n_p\kappa}\left(r\right), \\ Q_{n\kappa}\left(r\right)&=(-1)^l\sum_{n_q=1}^{n_{q\max}}d_{n_q\kappa}q_{n_q\kappa}\left(r\right), \end{aligned} \tag{10}$$

Here $(-1)^l$ insures the the inversion symmetry for the Dirac wave function (see [36] for a detailed explanation of the relativistic molecular symmetry spinors for diatomics). $p_{n_p\kappa}(r)$ and $q_{n_q\kappa}(r)$ are the normalized Slater type orbitals with non-integer principal quantum numbers (NISTOs):

$$\begin{aligned} p_{n_p\kappa}\left(r\right)&=\frac{\left(2\lambda_{p\kappa}\right)^{\gamma_\kappa+n_p-1/2}}{\sqrt{\Gamma\left(2\gamma_\kappa+2n_p-1\right)}}r^{\gamma_\kappa+n_p-2}\exp\left(-\lambda_{p\kappa}r\right), \\ q_{n_q\kappa}\left(r\right)&=\frac{\left(2\lambda_{q\kappa}\right)^{\gamma_\kappa+n_q-1/2}}{\sqrt{\Gamma\left(2\gamma_\kappa+2n_q-1\right)}}r^{\gamma_\kappa+n_q-2}\exp\left(-\lambda_{q\kappa}r\right), \end{aligned} \tag{11}$$

$\lambda_{p\kappa}>0$ and $\lambda_{q\kappa}>0$ are variational parameters. These functions satisfy the following uncoupled system of equations

$$\begin{aligned} \left[\frac{\partial}{\partial r}+\frac{1+\kappa}{r}\right]p_{n_p\kappa}\left(r\right)&=\left[-\lambda_{p\kappa}+\frac{\gamma_\kappa+n_p+\kappa-1}{r}\right]p_{n_p\kappa}\left(r\right), \\ \left[\frac{\partial}{\partial r}+\frac{1-\kappa}{r}\right]q_{n_q\kappa}\left(r\right)&=\left[-\lambda_{q\kappa}+\frac{\gamma_\kappa+n_q-\kappa-1}{r}\right]q_{n_q\kappa}\left(r\right). \end{aligned} \tag{12}$$

The non-integer parameter γ_κ is chosen from the asymptotic behavior of the large $P_{n\kappa}(r)$ and small $Q_{n\kappa}(r)$ components near the corresponding center

$$\gamma_\kappa=\gamma_{-\kappa}=\sqrt{\kappa^2-\frac{Z^2}{c^2}}. \tag{13}$$

The total Slater-type spinor function centered on a nucleus has the following compact form

$$\psi_{N_{\max}}\begin{pmatrix}\overrightarrow{r}\end{pmatrix}=\begin{cases}\imath\displaystyle\sum_{n=1}^{N_{\max}}\sum_{\kappa=-n,\,\kappa\neq0}^{n-1}P_{n\kappa}\left(r\right)\Omega_{+\kappa m}\left(\theta,\varphi\right), \\ \displaystyle\sum_{n=1}^{N_{\max}}\sum_{\kappa=-n,\,\kappa\neq0}^{n-1}Q_{n\kappa}\left(r\right)\Omega_{-\kappa m}\left(\theta,\varphi\right),\end{cases} \tag{14}$$

where $N_{\max}$ is a maximal principal quantum number, for which the highest powers of r $n_{p\max}, n_{q\max}$ given in Eq. (10) are chosen to avoid spurious solutions (described in the in the introduction) following [37].

$$n_{p\max}=n-|\kappa|+1, \quad n_{q\max}=\begin{cases}n_{p\max}, & \kappa<0, \\ n_{p\max}+1, & \kappa>0.\end{cases} \tag{15}$$

The total numbers of NISTOs depending on the $N_{\max}=2-5$ are presented in Table 1, where we can see that the total number of nonlinear parameters $\lambda_{p\kappa}$ and $\lambda_{q\kappa}$ is $2N_{\max}-1$, i.e. the one which brings the total number of nonlinear parameters to $4N_{\max}-2$.

The one-electron wave function $\Psi(\overrightarrow{r})$ for Eq. (1) has the form

$$\Psi(\overrightarrow{r})=\psi_{N_{\max}}(\overrightarrow{r}_1)+\psi_{N_{\max}}(\overrightarrow{r}_2), \tag{16}$$

for the $\Psi(\overrightarrow{r})=\Psi(-\overrightarrow{r})$ gerade case and

$$\Psi(\overrightarrow{r})=\psi_{N_{\max}}(\overrightarrow{r}_1)-\psi_{N_{\max}}(\overrightarrow{r}_2). \tag{17}$$

for the $\Psi(\overrightarrow{r})=-\Psi(-\overrightarrow{r})$ ungerade case with the condition $\langle\Psi(\overrightarrow{r})|\Psi(\overrightarrow{r})\rangle=1$. Finally, the minimax formulation [20] of the Dirac Eq. (1) is

$$-c^2\leqslant E_R=\min_{P_{n\kappa}(r)\neq0Q_{n\kappa}(r)}\max\left\langle H_D\right\rangle=\min_{\lambda_{p\kappa}}\max_{\lambda_{q\kappa}}\left\langle H_D\right\rangle\leqslant c^2. \tag{18}$$

Making the Rayleigh quotient (18) stationary with respect to the variations in $c_{n_p\kappa}$ and $d_{n_q\kappa}$, leads to the generalized eigenvalue problem

$$\mathbf{A}\begin{pmatrix}\mathbf{c}\\ \mathbf{d}\end{pmatrix}=E_R\mathbf{B}\begin{pmatrix}\mathbf{c}\\ \mathbf{d}\end{pmatrix}. \tag{19}$$

Table 1
Total numbers of NISTO depending on the maximal principal quantum number $N_{\max}$.

κ	States	$N_{\max}=2$		$N_{\max}=3$		$N_{\max}=4$		$N_{\max}=5$	
		$n_{p\max}$	$n_{q\max}$	$n_{p\max}$	$n_{q\max}$	$n_{p\max}$	$n_{q\max}$	$n_{p\max}$	$n_{q\max}$
- 1	$s_{1/2}$	2	2	3	3	4	4	5	5
1	$p_{1/2}$	2	3	3	4	4	5	5	6
- 2	$p_{3/2}$	1	1	2	2	3	3	4	4
2	$d_{3/2}$			2	3	3	4	4	5
- 3	$d_{5/2}$			1	1	2	2	3	3
3	$f_{5/2}$					2	3	3	4
- 4	$f_{7/2}$					1	1	2	2
4	$g_{7/2}$							2	3
- 5	$g_{9/2}$							1	1
Total number		11		24		41		62	

The determination of the matrix elements of $\langle\Psi(\vec{r})|\Psi(\vec{r})\rangle$ and the hamiltonian needs the determination of two center integrals such as

$$\begin{aligned} Q^{m_1m_2}_{l_1l_2}(a,\nu,\rho) &= \int d\vec{r}\, r_1^{-1} r_2^{\nu-1} e^{-ar_2} Y^*_{l_1m_1}\left(\vec{r}_2\right) Y_{l_2m_2}\left(\vec{r}_2\right) \\ &= (-1)^{l_1-l_2} \int d\vec{r}\, r_2^{-1} r_1^{\nu-1} e^{-ar_1} Y^*_{l_1m_1}\left(\vec{r}_1\right) Y_{l_2m_2}\left(\vec{r}_1\right), \end{aligned} \tag{20}$$

and

$$\begin{aligned} F^{m_1m_2}_{l_1l_2}(a_1,\nu_1,a_2,\nu_2,\rho) &= \int d\vec{r}\, r_1^{\nu_1-1} e^{-a_1r_1} Y^*_{l_1m_1}\left(\vec{r}_1\right) r_2^{\nu_2-1} e^{-a_2r_2} Y_{l_2m_2}\left(\vec{r}_2\right) \\ &= (-1)^{l_1-l_2} \int d\vec{r}\, r_2^{\nu_1-1} e^{-a_1r_2} Y^*_{l_1m_1}\left(\vec{r}_2\right) r_1^{\nu_2-1} e^{-a_2r_1} Y_{l_2m_2}\left(\vec{r}_1\right). \end{aligned} \tag{21}$$

Here a, a_1, a_2 are positive numbers; ν, ν_1, ν_2 are non-integer numbers; $\nu > -1, \max(\nu_1,\nu_2) > 0, \min(\nu_1,\nu_2) > -1$. Similar integrals are considered in [38–40], and evaluated in ellipsoidal coordinates in terms of the well-known auxiliary functions [41]. This approach requires many summations for high accuracy calculations, which depends on l_1, l_2, ν, ν_1 and ν_2. In the appendix we present our approach to the determination of these integrals.

3. Results

In all our calculations the mass of the electron $m_e = 1$, and the speed of light $c = 137.0359895$ both in atomic units. We determine, first of all, the relativistic energy E_R of the $1\sigma_g$ state of the lightest ion H_2^+. As, for light ions,the binding energy $E_e = E_R - c^2$ and the non-relativistic energy are close, we have chosen the initial estimates of the nonlinear parameters $\lambda_{p\kappa}, \lambda_{q\kappa}$ (11) for all κ

$$\lambda_{p\kappa} = \lambda_{q\kappa} = c^{-1}\sqrt{c^4 - E_R^2} \equiv c^{-1}\sqrt{-E_e(2c^2 + E_e)} \approx \sqrt{-2E_e}. \tag{22}$$

We have then calculated step-by-step the relativistic $1\sigma_g$ state energy E_R of the other ions, using the calculated $\lambda_{p\kappa}, \lambda_{q\kappa}$ during the previous step multiplied by the factor Z/Z_{old} as initial estimates. Here Z_{old} is the value of the charge in the previous step.

In Tables 2 and 3 are presented, the calculated relativistic $1\sigma_g$ state energy E_e for different ions at "chemical" internuclear distance $\rho = 2/Z$ versus the number $N_{\max}$ and compared to the results given in [25]. For the cases $N_{\max} = 2$ and $N_{\max} = 3$, we obtained the same relativistic energies with charge step 1 (i.e. $Z = 1,2,3,4,\ldots$) and with difference of charges presented in the Tables 2 and 3 (i.e. $Z = 1,2,10,20,\ldots$). For the case $N_{\max} = 4$ and $N_{\max} = 5$, there are many minimax solutions, so we calculated, first, the relativistic energies with the charge of step 1, then we recalculated it with different corrections of the nonlinear parameters $\lambda_{p\kappa}$ and $\lambda_{q\kappa}$.

From the results presented in Tables 2 and 3, we see that our calculated energies give the upper bounds of the exact energies with monotonic convergence with increasing $N_{\max}$. For $N_{\max} = 5$ our results are comparable to those [25] with a relative error of $10^{-7} - 10^{-8}$.

This verifies the validity of the approach given in [37] for the one-sided convergence of the minimax optimization under the condition (15). For $N_{\max} = 5$ we could identify the reason of having an spurious case. In fact checking the coefficients $c_{n_p\kappa}$ and $d_{n_q\kappa}$ in Eq. (10) we observed that, in some calculations $c_{n_q\kappa} \neq 0$ and $d_{n_q\kappa} = 0$ at $n_p = n_q = 5$, $\kappa = -1$. This means that the highest power of r in the large component is bigger than that of the small component. By correcting this anomaly we could avoid the spurious result.

Fig. 1 shows the scaled binding energy $Z^{-2}E_e$ in terms of the charge Z at the internuclear distance $\rho = 2/Z$. This shows how the electron is more and more bound to the nuclei. Note that the scaled non-relativistic binding energy $Z^{-2}E_e$ does not depend on the charge Z at the internuclear distance $\rho = 2/Z$.

In Fig. 2 we present the scaled relativistic energy $-1 < c^{-2}E_R < 1$ depending on the internuclear distance ρ and the charge $Z \geqslant 80$. Here the basis functions with $N_{\max} = 2$ are used. Also note that, for too small internuclear distances ρ, we can not calculate the relativistic energy, as we come very near to the one-center basis functions for which the fixed parameter $\gamma' = \sqrt{1 - (2Z)^2/c^2}$ for given Z (compare with (13)).

4. Conclusion

We have developed a new iterative scheme to obtain reliable solutions of the Dirac two center equation constructed by linear combinations of relativistic (non-integer) Slater type wave functions. We have used independent large and small components of the Dirac spinor. We present here the details of our original calculation of the two center

Table 2
The relativistic $1\sigma_g$ state energy $E_e = E_R - c^2$ at $\rho = 2/Z$.

Z	Ion	N_{max}	Energy	Energy [25]
		2	−1.102 248 990	
1	H_2^+	3	−1.102 624 606	
		4	−1.102 640 853	
		5	−1.102 641 574	−1.102 641 581
		2	−4.409 083 664	
2	He_2^{3+}	3	−4.410 586 724	
		4	−4.410 651 814	
		5	−4.410 654 700	−4.410 654 728
		2	−110.297 363 139	
10	Ne_2^{19+}	3	−110.335 418 709	
		4	−110.337 130 064	
		5	−110.337 203 677	−110.337 204 410
		2	−442.073 489 140	
20	Ca_2^{39+}	3	−442.231 839 925	
		4	−442.239 683 071	
		5	−442.239 984 905	−442.239 997 265
		2	−998.024 713 682	
30	Zn_2^{59+}	3	−998.404 961 752	
		4	−998.426 014 019	
		5	−998.426 773 718	−998.426 763 032
		2	−1782.802 217 068	
40	Zr_2^{79+}	3	−1783.539 606 894	
		4	−1783.585 615 512	
		5	−1783.587 315 610	−1783.587 355 445
		2	−2803.286 356 845	
50	Sn_2^{99+}	3	−2804.566 122 743	
		4	−2804.656 452 590	
		5	−2804.659 770 918	−2804.659 807 931
		2	−4069.063 950 398	
60	Nd_2^{119+}	3	−4071.139 360 212	
		4	−4071.304 123 628	
		5	−4071.309 804 433	−4071.309 830 161

integrals with non-integer powers of the position variables. Our approach permits to take control of the spurious solutions and avoid them by the appropriate choice of the wave function parameters. We investigate the electronic energy of $1\sigma_g$ orbitals with the nuclear charge Z. Our method can produce the solution for $1\sigma_u$ and higher levels which can be needed in the case of large internuclear distances to study the resonances between $1s\sigma_g$ and $1s\sigma_u$ close levels.

CRediT authorship contribution statement

O. Chuluunbaatar: Methodology, Software. **B.B. Joulakian:** Conceptualization, Writing, Editing. **G. Chuluunbaatar:** Software, Investigation. **J. Busa Jr.:** Software, Investigation. **G.O. Koshcheev:** Software, Investigation.

Declaration of Competing Interest

The authors declare that they have no known competing financial interests or personal relationships that could have appeared to influence the work reported in this paper.

Table 3
The relativistic $1\sigma_g$ state energy $E_e = E_R - c^2$ at $\rho = 2/Z$. Continuation of Table 2.

Z	Ion	N_{max}	Energy	Energy [25]
		2	−5593.251 717 146	
70	Yb_2^{139+}	3	−5596.462 436 297	
		4	−5596.746 534 092	
		5	−5596.754 858 416	−5596.754 864 752
		2	−7393.964 617 394	
80	Hg_2^{159+}	3	−7398.751 717 018	
		4	−7399.218 916 979	
		5	−7399.228 761 754	−7399.228 805 892
		2	−9497.103 757 814	
90	Th_2^{179+}	3	−9504.013 069 800	
		4	−9504.748 342 655	
		5	−9504.756 578 763	−9504.756 746 927
		2	−9957.149 867 657	
92	U_2^{183+}	3	−9964.557 040 570	
		4	−9965.357 892 685	
		5	−9965.365 278 947	−9965.365 468 058
		2	−11942.178 005 611	
100	Fm_2^{199+}	3	−11951.832 987 584	
		4	−11952.939 381 324	
		5	−11952.941 727 610	−11952.941 940 110
		2	−14796.324 879 456	
110	Ds_2^{219+}	3	−14809.322 202 267	
		4	−14810.852 901 248	
		5	−14810.898 911 675	
		2	−17461.232 762 069	
118	Og_2^{235+}	3	−17477.122 912 713	
		4	−17479.073 413 320	
		5	−17479.125 249 624	
		2	−18577.427 339 685	
121	$241+_2$	3	−18594.349 381 894	
		4	−18596.454 717 052	
		5	−18596.509 996 585	

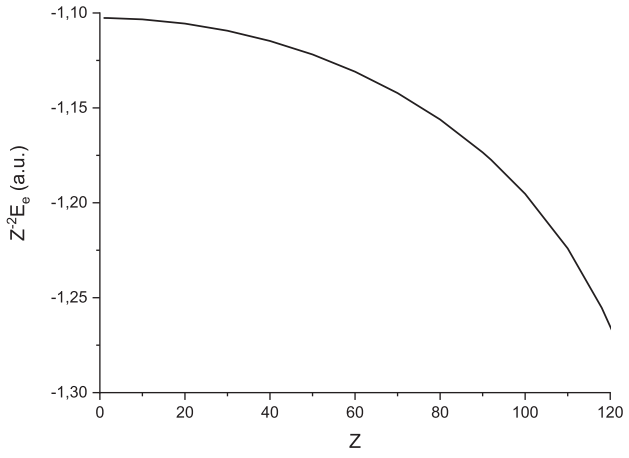

Fig. 1. The scaled binding energy $Z^{-2}E_e$ versus the charge Z at the internuclear distance $\rho = 2/Z$.

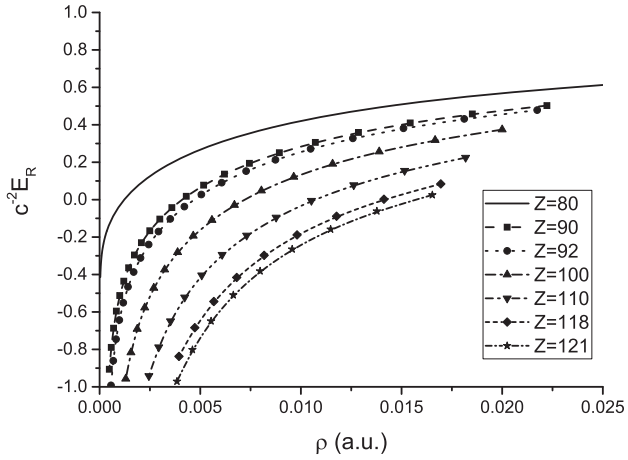

Fig. 2. The scaled relativistic energy $c^{-2}E_R$ versus the internuclear distance ρ and the charge $Z \geqslant 80$.

Acknowledgements

The authors would like to thank professor I.I. Tupitsyn for valuable discussions. Calculations were performed on the Central Information and Computer Complex and heterogeneous computing platform Hybri-LIT through supercomputer "Govorun" of JINR. This work was partially supported by the grant of Ministry of Science and Higher Education of the Russian Federation 075-10-2020-117.

Appendix A. Determination of the two-center integrals

$$\begin{aligned} Q^{m_1m_2}_{l_1l_2}(a,\nu,\rho) &= \int d\overrightarrow{r}\, r_1^{-1} r_2^{\nu-1} e^{-ar_2} Y^*_{l_1m_1}\left(\overrightarrow{r}_2\right) Y_{l_2m_2}\left(\overrightarrow{r}_2\right) \\ &= (-1)^{l_1-l_2} \int d\overrightarrow{r}\, r_2^{-1} r_1^{\nu-1} e^{-ar_1} Y^*_{l_1m_1}\left(\overrightarrow{r}_1\right) Y_{l_2m_2}\left(\overrightarrow{r}_1\right), \end{aligned} \tag{A.1}$$

and

$$\begin{aligned} F^{m_1m_2}_{l_1l_2}(a_1,\nu_1,a_2,\nu_2,\rho) &= \int d\overrightarrow{r}\, r_1^{\nu_1-1} e^{-a_1r_1} Y^*_{l_1m_1}\left(\overrightarrow{r}_1\right) r_2^{\nu_2-1} e^{-a_2r_2} Y_{l_2m_2}\left(\overrightarrow{r}_2\right) \\ &= (-1)^{l_1-l_2} \int d\overrightarrow{r}\, r_2^{\nu_1-1} e^{-a_1r_2} Y^*_{l_1m_1}\left(\overrightarrow{r}_2\right) r_1^{\nu_2-1} e^{-a_2r_1} Y_{l_2m_2}\left(\overrightarrow{r}_1\right). \end{aligned} \tag{A.2}$$

Here a, a_1, a_2 are positive numbers; ν, ν_1, ν_2 are non-integer numbers; $\nu > -1, \max(\nu_1,\nu_2) > 0, \min(\nu_1,\nu_2) > -1$. We use the Fourier transform

$$Q^{m_1m_2}_{l_1l_2}\left(a,\nu,\rho\right) = 8 \sum_{l=|l_1-l_2|,2}^{l_1+l_2} (-1)^l Y_{l0}\left(\overrightarrow{\rho}\right) \Upsilon^{0m_1m_2}_{ll_1l_2} \int_0^\infty dp j_l\left(p\rho\right) g_l\left(a,\nu,p\right), \tag{A.3}$$

$$\begin{aligned} F^{m_1m_2}_{l_1l_2}\left(a_1,\nu_1,a_2,\nu_2,\rho\right) &= 8 \sum_{l=|l_1-l_2|,2}^{l_1+l_2} (-1)^{\frac{3l+l_1-l_2}{2}} Y_{l0}\left(\overrightarrow{\rho}\right) \Upsilon^{0m_1m_2}_{ll_1l_2} \\ &\times \int_0^\infty dp p^2 j_l\left(\rho p\right) g_{l_1}\left(a_1,\nu_1,p\right) g_{l_2}\left(a_2,\nu_2,p\right), \end{aligned} \tag{A.4}$$

where

$$\Upsilon^{mm_1m_2}_{ll_1l_2} = \int d\Omega_p Y_{lm}\left(\overrightarrow{p}\right) Y^*_{l_1m_1}\left(\overrightarrow{p}\right) Y_{l_2m_2}\left(\overrightarrow{p}\right), \tag{A.5}$$

which has a non-zero value for

$$m = m_2 - m_1, \quad l = |l_1-l_2|, |l_1-l_2|+2, \ldots, l_1+l_2. \tag{A.6}$$

Here the sign * denotes the complex conjugate, and $j_l(p)$ is a spherical Bessel function [42]. The integral (A.5) is calculated analytically using the Clebsch-Gordan coefficients. It can also be calculated directly using MAPLE without loss of precision. The function $g_l(a,\nu,p)$ has the form

$$g_l\left(a,\nu,p\right) = \int_0^\infty dr r^{\nu+1}\exp\left(-ar\right)j_l\left(pr\right), \quad \nu > -2. \tag{A.7}$$

Using the following relation for the integral of the product of two spherical Bessel functions [43]

$$\int_0^\infty dp j_l\left(p\rho\right)j_l\left(pr\right) = \frac{\pi}{2(2l+1)}\begin{cases}\rho^{-l-1}r^l, & \rho \geqslant r,\\ \rho^l r^{-l-1}, & \rho < r,\end{cases} \tag{A.8}$$

we obtain

$$\begin{aligned}\int_0^\infty dp j_l\left(p\rho\right)g_l\left(a,\nu,p\right) &= \int_0^\infty dr r^{\nu+1}\exp\left(-ar\right)\int_0^\infty dp j_l\left(p\rho\right)j_l\left(pr\right)\\ &= \frac{\pi}{2(2l+1)}\left(\frac{1}{\rho^{l+1}}\int_0^\rho dr r^{\nu+l+1}\exp\left(-ar\right) + \rho^l\int_\rho^\infty dr r^{\nu-l}\exp\left(-ar\right)\right)\\ &= \frac{\pi}{2(2l+1)a^{\nu+1}}\left(\frac{1}{(a\rho)^{l+1}}\gamma\left(\nu+l+2,a\rho\right) + (a\rho)^l\Gamma\left(\nu-l+1,a\rho\right)\right),\end{aligned} \tag{A.9}$$

where $\Gamma(a,x)$ and $\gamma(a,x)$ are respectively the upper and lower incomplete gamma functions [42]. This permits the analytical calculation of the integral in (A.3).

Now let us consider the integral (A.4), which will be calculated numerically. Using the following recurrence relations of the spherical Bessel function [42]

$$j_l\left(pr\right) = \frac{(2l-1)}{pr}j_{l-1}\left(pr\right) - j_{l-2}\left(pr\right) = \frac{l-1}{pr}j_{l-1}\left(pr\right) - \frac{1}{p}\frac{d}{dr}j_{l-1}\left(pr\right), \tag{A.10}$$

we obtain the following recurrence relations for the integral (A.7)

$$\begin{aligned}g_l(a,\nu,p) &= \frac{(2l-1)}{p}g_{l-1}\left(a,\nu-1,p\right) - g_{l-2}\left(a,\nu,p\right)\\ &= \frac{l+\nu}{p}g_{l-1}\left(a,\nu-1,p\right) - \frac{a}{p}g_{l-1}\left(a,\nu,p\right)\\ &= \frac{a}{p}\frac{2l-1}{\nu-l+1}g_{l-1}\left(a,\nu,p\right) - \frac{l+\nu}{\nu-l+1}g_{l-2}\left(a,\nu,p\right)\end{aligned} \tag{A.11}$$

with

$$g_0\left(a,\nu,p\right) = \frac{\Gamma(\nu+1)}{p}\Im\left(\frac{1}{(a-ip)^{\nu+1}}\right) = \frac{\Gamma(\nu+1)}{p\sqrt{(a^2+p^2)^{\nu+1}}}\sin\left(\left(\nu+1\right)\arcsin\left(\frac{p}{\sqrt{a^2+p^2}}\right)\right). \tag{A.12}$$

Also the integral (A.7) can be expressed analytically using the relation between the spherical and cylindrical Bessel functions, and the formula 6.621.1 in [43]

$$g_l\left(a,\nu,p\right) = \frac{p^l}{\sqrt{(a^2+p^2)^{l+\nu+2}}}\frac{\Gamma(l+\nu+2)}{(2l+1)!!}{}_2F_1\left(\frac{l+\nu+2}{2},\frac{l-\nu}{2};l+\frac{3}{2};\frac{p^2}{a^2+p^2}\right), \tag{A.13}$$

where ${}_2F_1(a,b;c;z)$ is a hypergeometric function [42]. From here, we can obtain the following asymptotic behaviors for the small and large values of p

$$g_l(a,\nu,p) \sim p^l, \quad p\to 0; \quad g_l(a,\nu,p) \sim p^{-\nu-2}, \quad p\to\infty. \tag{A.14}$$

Taking into account (A.14), the integrand in the p integration (A.4) behaves like

$$p^2 j_l\left(\rho p\right)g_{l_1}\left(a_1,\nu_1,p\right)g_{l_2}\left(a_2,\nu_2,p\right) \sim \begin{cases}p^{l+l_1+l_2+2}, & r\to 0,\\ p^{-s}\sin\left(\rho p - \frac{l\pi}{2}\right), & r\to\infty,\end{cases} \tag{A.15}$$

with $s = \nu_1 + \nu_2 + 3 > 2$.

The following **Algorithm** is used to calculate the integral (A.4) numerically with high accuracy.

1. In most cases, the integral over p is calculated for each l, and summed over. We represent (A.4) in the form

$$F^{m_1 m_2}_{l_1 l_2}\left(a_1,\nu_1,a_2,\nu_2,\rho\right) = 8\int_0^\infty dpp^2 g_{l_1}\left(a_1,\nu_1,p\right) g_{l_2}\left(a_2,\nu_2,p\right) f\left(p,\rho\right),$$
$$f\left(p,\rho\right) = \sum_{l=|l_1-l_2|,2}^{l_1+l_2} (-1)^{\frac{3l+l_1-l_2}{2}} Y_{l0}\left(\overrightarrow{\rho}\right) \Upsilon^{0m_1m_2}_{ll_1l_2} j_l\left(\rho p\right), \tag{A.16}$$

i.e., first sum over l, then integrate over p. This avoids multiple recalculations of the functions $g_{l_1}(a_1,\nu_1,p), g_{l_2}(a_2,\nu_2,p)$ for each value l.

2. We divide the integration interval into two parts $[0,b]$ and $[b,\infty]$, where $b \geqslant \pi/\rho$ is a first zero of $j_{|l_1-l_2|}(\rho p)$. The first integral can be calculated using high-order Gauss-Kronrod or Gauss-Legendre quadrature formulas. To calculate the second integral we use the explicit definition of the spherical Bessel functions

$$j_l\left(z\right) = \sin\left(z-\frac{\pi l}{2}\right)\sum_{k=0}^{\lfloor l/2\rfloor}(-1)^k\frac{h_{2k}}{z^{2k+1}} + \cos\left(z-\frac{\pi l}{2}\right)\sum_{k=0}^{\lfloor (l-1)/2\rfloor}(-1)^k\frac{h_{2k+1}}{z^{2k+2}}, \tag{A.17}$$

where $\lfloor x\rfloor$ is the integer part of x, and h_j are independent numbers from z. In this case we can represent the second integral in the form

$$\int_b^\infty dpp^2 g_{l_1}\left(a_1,\nu_1,p\right) g_{l_2}\left(a_2,\nu_2,p\right)\left[s\left(p,\rho\right)\sin\left(\rho p\right) + c\left(p,\rho\right)\cos\left(\rho p\right)\right]. \tag{A.18}$$

To calculate the above integral we use the algorithm, which is described in [44] and the routine QAWFE [45]. Note that the routine QAWFE evaluates the above integral separately with the factors $\sin(\rho p)$ and $\cos(\rho p)$. To avoid recalculation of the functions $g_{l_1}(a_1,\nu_1,p), g_{l_2}(a_2,\nu_2,p)$, we modified the routine QAWFE to evaluate the integral with both factors $\sin(\rho p)$ and $\cos(\rho p)$.

3. Many functions, like $g_{l_i}(a_i,\nu_i,p_i)$ are needed for the same combination of input arguments. Since the nature of the parameters (their range and distribution) were not clear in advance, we have created a structure of a linked list of trees based on an AVL-tree [46], where each tree represents one set of parameters. We begin by searching for the first parameter (e.g., a_i) going through the first tree starting from the head l_i. After finding the leaf containing the parameter a_i, we move to the next tree to which it points, searching for the parameter ν_i. After finding the parameter ν_i, we move to the next level and start to search for the last parameter p_i. Finding the last parameter p_i we have found the node containing the function for this combination of parameters. It takes $\mathscr{O}(\log n)$ operations to find one parameter in a tree, n being number of unique values of a given parameter. In our case, since the number of combinations for each set of parameters is rather small about 1 to 2 comparisons are sufficient to find given parameter. As this approach resulted in a significant speedup of the calculation, it was employed also for other functions.

We have the generalized eigenvalue problem (19) with an ill-conditioned mass matrix **B** (for example the condition number is $\sim 10^8$ at $N_{\max} = 5$), so all integrals are calculated with an accuracy of 10^{-20}, and used quadruple precision arithmetic.

The efficiency of the above **Algorithm** is confirmed by numerical experiments. For example if $N_{\max} = 5$, the total calculation time of all matrix elements using Steps 1 and 2 is approximately 4.5 times less than directly by formula (A.4) (i.e., the integral over p is first calculated for fixed l, and then summed over l) using only Step 2, with separate calculations for the part with $\sin(\rho p)$ and $\cos(\rho p)$. With the additional use of Step 3, the total calculation time is approximately 5 times less than when only Steps 1 and 2 are used. For $N_{\max} = 5$, the computational time for one iteration (including calculations of the energy, the corresponding gradient and the Hessian) on the supercomputer "Govorun" (Intel® Xeon® Platinum 8268, 24 cores, 2.9 GHz) is approximately 12 min.

References

[1] L.I. Ponomarev, T.P. Puzynina, Sov. Phys. JETP 25 (1967) 846–852.
[2] M. Aubert, N. Bessis, G. Bessis, Phys. Rev. A 10 (1974) 51–60, and references therein.
[3] C.A. Coulson, A. Joseph, Int. J. Quant. Chem. 1 (1967) 337–347.
[4] M.H. Johnson, B.A. Lippmann, Phys. Rev. 78 (1950) 329 (A).
[5] M.S. Marinov, V.S. Popov, Sov. Phys. JETP 41 (1975) 205–209.
[6] K. Rumrich, G. Soff, W. Greiner, Phys. Rev. A 47 (1993) 215–228.
[7] M. Gail, N. Grün, W. Scheid, J. Phys. B 36 (2003) 1397–1407.
[8] O.O. Sobol, E.V. Gorbar, V.P. Gusynin, Phys. Rev. B 88 (2013) 205116-1–205116-9.
[9] A. De Martino, D. Klöpfer, D. Matrasulov, R. Egger, Phys. Rev. Lett. 112 (2014) 186603-1–186603-5.
[10] O.O. Sobol, Ukrainian J. Phys. 59 (5) (2014) 531–540.
[11] E.V. Gorbar, V.P. Gusynin, O.O. Sobol, EPL 111 (2015) 37003-1–37003-6.
[12] O.O. Sobol, Ukrainian J. Phys. 61 (5) (2016) 759–773.
[13] D. Klöpfer, A. De Martino, D.U. Matrasulov, R. Egger, Eur. Phys. J. B 87 (2014) Article number: 187-1-9.
[14] E.V. Gorbar, V.P. Gusynin, O.O. Sobol, Low Temp. Phys. 44 (2018) 371–400.
[15] P.I. Pavlik, S.M. Blinder, J. Chem. Phys. 46 (1967) 2749–2751.
[16] B. Muller, J. Rafelski, W. Greiner, Phys. Lett. 47B (1973) 5–7.
[17] F. Mark, U. Becker, Physica Scipta 36 (1987) 393–396.
[18] F.A. Parpia, A.K. Mohanty, Chem. Phys. Lett. 238 (1995) 209–214.
[19] P.P. Gorvat, V.Yu. Lazur, S.I. Migalina, I.M. Shuba, P.K. Yanev, Theor. Math. Phys. 109 (1996) 1423–1436.
[20] J.D. Talman, Phys. Rev. Lett. 57 (1986) 1091–1094.
[21] L. LaJohn, J.D. Talman, Theor. Chem. Acc. 99 (1998) 351–356.
[22] A. Ishikawa, H. Nakashima, H. Nakatsuji, J. Chem. Phys 128 (2008) 124103-1–124103-14.
[23] O. Kullie, D. Kolb, Eur. Phys. J. D 17 (2001) 167–173.
[24] A.N. Artemyev, A. Surzhykov, P. Indelicato, G. Plunien, Th. Stöhlker, J. Phys. B 43 (2010) 235207-1–235207-8.
[25] I.I. Tupitsyn, D.V. Mironova, Opt. Spectrosc. 117 (2014) 351–357.
[26] W.R. Johnson, S.A. Blundell, J. Sapirstein, Phys. Rev. A 37 (1988) 307–315.
[27] A. Kolakowska, J. Phys. B 29 (1996) 4515–4527.
[28] V.M. Shabaev, I.I. Tupitsyn, V.A. Yerokhin, G. Plunien, G. Soff, Phys. Rev. Lett. 93 (2004) 130405-1–130405-4.
[29] W.R. Johnson, K.T. Cheng, M.H. Chen, Theor. Comput. Chem. 14 (2004) 120–187.
[30] J.L. Zhou, A.L. Tits, Technical Research Report, TR-92-107 (1992).
[31] P.E. Gill, W. Murray, Math. Program. 7 (1974) 311–350.
[32] M.A. Howe, A quasi-newton algorithm for continuous minimax with applications to risk management in finance (PhD thesis of), The University of London, 1994.
[33] L. Adolphs, H. Daneshmand, A. Lucchi, Th. Hofmann, arXiv:1805.05751 (2018).
[34] I.V. Puzynin, T.L. Boyadjiev, S.I. Vinitsky, E.V. Zemlyanaya, T.P. Puzynina, O. Chuluunbaatar, Phys. Part. Nucl. 38 (2007) 70–116.
[35] E.U. Condon, G.H. Shortley, The Theory of Atomic Spectra, Cambridge at the University Press, 1970.
[36] J. Oreg, G. Malli, J. Chem. Phys. 61 (1974) 4349–4356.

[37] A. Kolakowska, J.D. Talman, K. Aashamar, Phys. Rev. A. 53 (1996) 168–177.
[38] T. Özdoğan, M. Orbay, S. Gümüş, Commun. Theor. Phys. (Beijing, China) 37 (2002) 711–714.
[39] A. Bağci, P.E. Hoggan, Phys. Rev. E 89 (2014) 053307-1–053307-7.
[40] A. Bağci, Rend. Fis. Acc. Lincei 31 (2020) 369–385.
[41] I.I. Guseinov, B.A. Mamedov, M. Kara, M. Orbay, Pramana-J. Phys. 56 (2001) 691–696.
[42] M. Abramovits, I.A. Stegun, Handbook of Mathematical Functions, Dover, New York, 1972.
[43] I.S. Gradshteyn, I.M. Ryzhik, Table of Integrals, Series, and Products, seventh ed., Academic Press is an imprint of Elsevier, 2007.
[44] R. Piessens, E. de Doncker-Kapenga, C. Überhuber, D. Kahaner, QUADPACK, A Subroutine Package for Automatic Integration, Springer-Verlag, 1983.
[45] http://www.netlib.org/quadpack.
[46] G. Adelson-Velsky, E. Landis, Proceedings of the USSR Academy of Sciences (in Russian) 146, 263–266; English translation by Myron, J. Ricci Soviet Math. Doklady 3 (1962) 1259–1263.